

A Unified Model for Non-Fickian Diffusion and Anomalous Swelling of Glassy Polymer Gels

Peihan Lyu,¹ Zhaoyu Ding,¹ Masao Doi,^{1,2,*} and Xingkun Man^{1,3,†}

¹*School of Physics, Beihang University, Beijing 100191, China*

²*Wenzhou Institute, University of Chinese Academy of Sciences, Wenzhou 325000, China*

³*Peng Huanwu Collaborative Center for Research and Education, Beihang University, Beijing 100191, China*

A sheet of glassy polymers placed in solvent shows swelling behaviors quite different from that of soft polymers (rubbers and gels). (1) Non-Fickian diffusion (called case II diffusion): As solvent permeates into the sample, a sharp front is created between the swollen part and the glassy part, and it moves towards the center at constant speed. (2) Non-monotonous swelling: The thickness of the sample first increases and then decreases towards the equilibrium value. Here we propose a theory to explain such anomalous behavior by extending the previous theory for swelling of soft gels. We regard the material as a continuum mixture of glassy polymer network and solvent. We assume that the polymer network is a viscoelastic gel of glassy polymers and its relaxation time depends strongly on solvent concentration. We will show that this theory explains the above two characteristics of glassy polymers in a simple and unified framework. The theory predicts how the permeation speed of solvent and the characteristic times of the swelling process depend on material parameters and experimental conditions, which can be checked experimentally.

When a thin sample of polymer is placed in a bath of solvent, the solvent permeates into the polymer and increases the volume of the sample. In soft polymers (rubbers and gels), the thickness and the area of the sample increase monotonically in time t , following the Fickian diffusion law (in proportion to $t^{1/2}$) and reach the equilibrium value. On the other hand, in glassy polymer, the swelling behavior is completely different [1–6]. In the classical experiment, Thomas and Windle [1] reported the following anomalies in the swelling of PMMA (poly-methyl-methacrylate) sheet in methanol (see Fig.1). (a) At first, as the solvent permeates into the polymer, a soft rubbery part is created at the surface of the polymer and moves towards the center. During this process, the interface between the rubbery part and the glassy part remains sharp, and it moves at constant speed. At this stage, the sample thickness increases in time in proportion to t , while the sample width remains constant. (b) After some time, the two fronts created at both surfaces meet at the center and the whole polymer becomes rubbery. At this stage, the thickness decreases in time while the width increases towards their equilibrium values.

The non-Fickian diffusion dynamics characterizing the first stage is observed for many glassy polymers, and is called case II diffusion [7–12]. The case II diffusion is characterized by the existence of sharp front of swollen region that moves at constant speed. Such behavior is considered to be caused by the glass transition of polymers induced by solvent. Numerous theories have been proposed to describe the case II diffusion [13–19]. However, there is still no consensus or clear understanding on how the case II behavior is caused by the glass transition.

All previous theories have a common drawback that they only discuss the one dimensional problem of diffusion in the first stage [20–28]. Such theory cannot discuss the three dimensional problem of shape change in the

second stage and how the first stage transforms to the second stage. To deal with the second stage, separate theory was needed.

In this paper, we propose a three dimensional theory for the swelling of glassy polymer. We regard the glassy polymer as a viscoelastic gel of glassy polymer and discuss its swelling using the same framework as that for the soft polymer gels [29–32]. We take the conventional view for glass transition, and assume that the kinetic parameters (solvent diffusion constants and polymer relaxation times) change by orders of magnitude at some characteristic solvent volume fraction. We shall show that this simple model reproduces the two anomalies, the case II

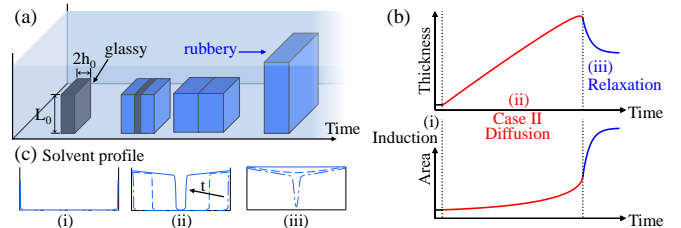


FIG. 1. (a) Schematic of the swelling of a square sheet of glassy polymers in a bath of solvent. The sheet initially has side length L_0 and thickness $2h_0$ ($h_0 \ll L_0$). As solvent permeates, sharp front is formed between outer rubbery part (blue) and inner glassy part (black). After some time, the entire sample becomes rubbery, relaxing towards the equilibrium state. (b) Time evolution of thickness (top) and area (bottom) show three stages. (i) Induction stage (black): both thickness and area are nearly unchanged. (ii) Case II diffusion stage (red): thickness increases in time in proportion to t , while area nearly remains constant. (iii) Relaxation stage (blue): thickness decreases but area increases towards the equilibrium value. (c) Time evolution of the solvent profile along z -axis in the three stages.

diffusion and the non-monotonous shape change without introducing any additional assumptions.

We consider a square sheet of glassy polymer gel that is initially homogeneous and isotropic with thickness $2h_0$ and side length L_0 ($h_0 \ll L_0$), (see Fig.1). We take a Cartesian coordinate such that the right and the left surfaces are at $z = \pm h_0$. Suppose that a point located at \mathbf{r} on the polymer network in the dry state is displaced to $\mathbf{r} + \mathbf{u}(\mathbf{r}, t)$ at time t . We use a homogeneous continuum model and assume that the displacement gradient $\varepsilon_{\alpha\beta} = \partial u_\alpha / \partial r_\beta$ (α, β stand for x, y, z) is small, and that the swelling takes place uniformly and isotropically in x - y plane. The displacement vector can be written as $u_x(t) = \alpha(t)x$, $u_y(t) = \alpha(t)y$, and $u_z = u(z, t)$, where $\alpha(t)$ and $u(z, t)$ are the unknowns to be obtained.

For small deformation, the polymer velocity \mathbf{v}_p at \mathbf{r} is given by the time derivative of $\mathbf{u}(\mathbf{r}, t)$, i.e. $\mathbf{v}_p = \dot{\mathbf{u}}$. The solvent velocity \mathbf{v}_s is different from \mathbf{v}_p and the difference represents the diffusion (or permeation) of solvent in polymer network. We assume that the system is incompressible as a whole, and always take the dry state as the reference state. This allows us to write the volume fraction of solvent ϕ_s in terms of the volume expansion of polymer network as $\phi_s = \nabla \cdot \mathbf{u} = \partial u / \partial z + 2\alpha$. Therefore, the state of the sample at time t is completely characterized by $u(z, t)$ and $\alpha(t)$.

To determine the time evolution of $u(z, t)$ and $\alpha(t)$, we use Onsager principle, which states that their evolution rate \dot{u} and $\dot{\alpha}$ are determined by the minimum of the Rayleighian function defined by $\mathfrak{R} = \dot{F} + \Phi$. Here, \dot{F} is the time derivative of free energy F , and Φ is the energy dissipation function of the system [33, 34].

The free energy F includes elastic energy of polymer network and mixing energy of polymer and solvent. For small deformation, the free energy is given in the same form as in soft gels [30, 31]

$$\frac{F}{L_0^2} = \int_0^{h_0} dz \left[\frac{K}{2} \left(2\alpha + \frac{\partial u}{\partial z} - 3\varepsilon_{\text{eq}} \right)^2 + \frac{2G}{3} \left(\frac{\partial u}{\partial z} - \alpha \right)^2 \right] \quad (1)$$

where ε_{eq} is the equilibrium strain, and K and G are the material constants called osmotic bulk modulus and shear modulus, respectively.

The energy dissipation function has two parts. (a) Φ_{dif} which arises from the friction between polymer and solvent. This term is given by the same as that for soft gels $\Phi_{\text{dif}} = \int d\mathbf{r} \frac{\xi}{2} (\mathbf{v}_p - \mathbf{v}_s)^2$, where ξ is the friction coefficient. (b) Φ_{rhe} which arises from the configurational change of the polymer. This is a new term introduced in the present theory to account for the glass transition. In polymeric materials, the glass transition is a rheological transition and has been represented by a very large change of rheological relaxation time across the transition point [35]. To account for this effect, we model the polymer network of glassy gel by the Kelvin-Voigt model for viscoelastic solid. This model

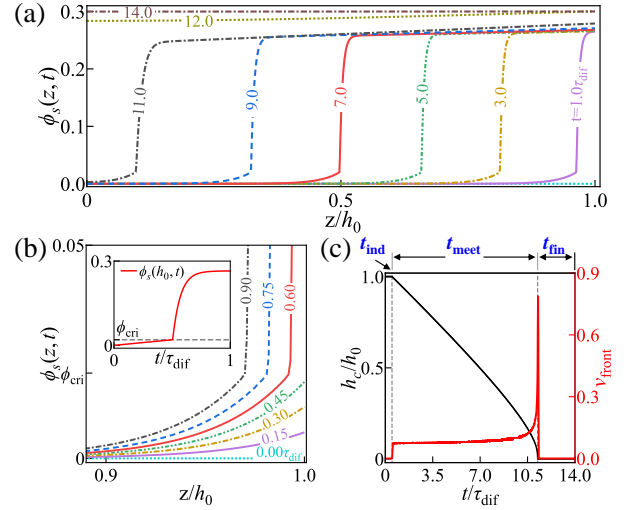


FIG. 2. (a) Time evolution of the solvent volume fraction $\phi_s(z, t)$ in the swelling of a sample which includes no solvent at time $t = 0$, i.e., $\phi(z, 0) = 0$. (b) Zoomed-in view of (a) in the region near the surface at early time of permeation. The inset is the time dependence of solvent volume fraction at gel surface $\phi_s(h_0, t)$. (c) Time dependence of the front position $h_c(t)$ and the front velocity v_{front} , indicating three characteristic periods: (i) induction period, t_{ind} , during which $h_c(t)$ remains unchanged at the surface, (ii) case II diffusion period, t_{meet} , during which h_c moves towards the center at a nearly constant speed, and (iii) relaxation period t_{fin} , during which h_c decreases to zero. All times are scaled by $\tau_{\text{dif}} = h_0^2/D_r$. Other parameters are $\xi_g/\xi_r = 5000$, $\eta_g/\eta_r = 100$ and $\eta_r/\xi_r h_0^2 = 0.05$.

is derived from the energy dissipation function $\Phi_{\text{rhe}} = \int d\mathbf{r} \frac{\eta}{4} \sum_{\alpha\beta} \left(\dot{\varepsilon}_{\alpha\beta} + \dot{\varepsilon}_{\beta\alpha} - \frac{2}{3} \delta_{\alpha\beta} \sum_\gamma \dot{\varepsilon}_{\gamma\gamma} \right)^2$ [36]. Here η is a material parameter called internal viscosity, which is defined by the rheological relaxation time τ_{rhe} as $\eta = G\tau_{\text{rhe}}$.

Our model includes two kinetic parameters ξ and η : ξ represents the dissipation due to the relative motion between polymer and solvent, and η represents the dissipation due to the conformational change of the polymer. We assume that they change by orders of magnitude at some solvent volume fraction ϕ_{cri} . Specifically, we assume that ξ and η depend on ϕ_s as $\xi(\phi_s) = \xi_r + \frac{1}{2} (\xi_g - \xi_r) \left(1 + \tanh \frac{\phi_{\text{cri}} - \phi_s}{\phi_w} \right)$ and $\eta(\phi_s) = \eta_r + \frac{1}{2} (\eta_g - \eta_r) \left(1 + \tanh \frac{\phi_{\text{cri}} - \phi_s}{\phi_w} \right)$, where ξ_g and η_g (ξ_r and η_r) are the friction coefficient and viscosity in the glassy state (rubbery state), and ϕ_w is the width of the glass transition region. On the other hand, we assume that the modulus K and G are constants independent of ϕ_s .

For the present problem, the energy dissipation func-

tion $\Phi = \Phi_{\text{dif}} + \Phi_{\text{rhe}}$ is written as [36]

$$\frac{\Phi}{L_0^2} = \int_0^{h_0} dz \left[\frac{\xi(\phi_s)}{2} (\dot{u} + 2\dot{\alpha}z)^2 + \frac{2\eta(\phi_s)}{3} \left(\frac{\partial \dot{u}}{\partial z} - \dot{\alpha} \right)^2 \right] \quad (2)$$

The Rayleighian of the system is given by $\mathfrak{R} = \Phi + \dot{F}$. The minimum condition of the Rayleighian gives the following set of equations[36]. Time evolution equation,

$$\xi(\dot{u} + 2\dot{\alpha}z) = \left(K + \frac{4}{3}G \right) \frac{\partial^2 u}{\partial z^2} + \frac{4}{3} \frac{\partial}{\partial z} \left[\eta \left(\frac{\partial \dot{u}}{\partial z} - \dot{\alpha} \right) \right] \quad (3)$$

$$G(u - \alpha h_0) + \int_0^{h_0} \eta \left(\frac{\partial \dot{u}}{\partial z} - \dot{\alpha} \right) dz = 0 \quad (4)$$

and the boundary condition at $z = h_0$

$$\frac{4}{3}\eta(\dot{\phi}_s - 3\dot{\alpha}) + K(\phi_s - 3\varepsilon_{\text{eq}}) + \frac{4}{3}G(\phi_s - 3\alpha) = 0 \quad (5)$$

Equations (3) and (4) are the set of equations which describe the swelling process of glassy polymers.

Equation (3) indicates that the motion in z direction is determined by two terms, the diffusion term $(K + \frac{4}{3}G) \frac{\partial^2 \phi_s}{\partial z^2}$ and the viscosity term $\frac{4}{3} \frac{\partial}{\partial z} [\eta(\dot{\phi}_s - 3\dot{\alpha})]$. The diffusion pushes solvent towards glassy region, but the internal viscosity hinders such permeation.

The boundary condition (5) is automatically derived from the variational calculus. It represents the condition that the normal stress acting on the polymer network at $z = h_0$ is zero. This boundary condition is quite different from the usual Neuman condition for soft gels [30, 31], and plays an important role in the subsequent discussions. Due to the symmetry of the system, we use the boundary condition $\partial u(z, t)/\partial z = 0$ at $z = 0$;

We solved eqs. (3)-(5) numerically, and calculated the time variation of the solvent volume fraction $\phi_s(z, t) = \partial u/\partial z + 2\alpha$, the thickness change $\Delta h(t) = u(h_0, t)$ and the area change $2L_0^2\alpha(t)$.

We first study the system that initially there is no solvent in sample, i.e. the initial value of the volume fraction of solvent ϕ_0 is equal to 0.

Figure 2(a) shows the time evolution of the solvent volume fraction $\phi_s(z, t)$ obtained by the numerical calculation. Here $\tau_{\text{dif}} = h_0^2/D_r$ with $D_r = (K + \frac{4}{3}G)/\xi_r$, represents the characteristic swelling time [37] of the gel in rubbery region and is taken to be the unit of time in this paper. It is seen that the solvent permeation proceeds with characteristic step-function shape: the glassy region where $\phi_s(z, t)$ is less than ϕ_{cri} and the rubbery region where $\phi_s(z, t)$ is much larger than ϕ_{cri} . The interface between the two regions is sharp. To see the motion of the interface, we define the front position $h_c(t)$ as the point where $\phi_s(z, t)$ is equal to ϕ_{cri} , and plotted $h_c(t)$ and its time derivative, i.e., the front velocity $v_{\text{front}} = \dot{h}_c(t)$, as a function of time in Figure 2(c).

In the beginning, there is no rubbery region and we define the front at the surface, i.e., $h_c(t) = h_0$. At the late

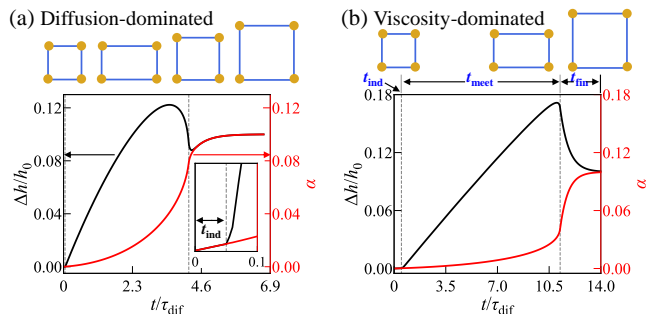


FIG. 3. Time dependence of the two strains $\Delta h(t)/h_0$ (black solid line) and $\alpha(t)$ (red solid line) for glassy polymers with (a) lower viscosity ($\eta_r/\xi_r h_0^2 = 0.005$) and (b) higher viscosity ($\eta_r/\xi_r h_0^2 = 0.05$). The top figure shows schematic time evolution of the apparent shape of the sample. The last stage in (a) is diffusion-dominated and in (b) is viscosity-dominated. Other parameters are the same as in Fig. 2.

stage of swelling, the glassy region disappears, and we define $h_c(t) = 0$. In the following, we call the first period in which there is no rubbery region induction period, and denote its duration time with t_{ind} . We call the last stage in which there is no glassy region, the relaxation period, and denote its duration time by t_{fin} . We shall call the period between these two stages as the case II period, and denote its duration time by t_{meet} . We now discuss each period in more detail.

Induction period. Figure 2(b) shows the evolution of $\phi_s(z, t)$ in short time after the swelling starts. It is seen that in the induction period where $\phi_s(z, t)$ is less than ϕ_{cri} , $\phi_s(z, t)$ evolves as in standard diffusion. This can be understood as follows. In the induction period, ξ and η in eq. (3) are equal to ξ_g and η_g and are constant. Furthermore, $\alpha(t)$ is close to the initial value $\phi_0/3 = 0$, and can be ignored. Therefore eq. (3) reduces to the following linear equation for $\phi_s(z, t)$.

$$\xi_g \dot{\phi}_s = \left(K + \frac{4}{3}G \right) \frac{\partial^2 \phi_s}{\partial z^2} + \eta_g \frac{4}{3} \frac{\partial^2 \dot{\phi}_s}{\partial z^2} \quad (6)$$

Equation (6) can be solved by Fourier-Laplace transform under the boundary condition (5), which is now simplified as

$$\frac{4}{3}\eta(\phi_s)\dot{\phi}_s + K(\phi_s - \phi_{\text{eq}}) + \frac{4}{3}G\phi_s = 0 \quad (7)$$

where $\phi_{\text{eq}} = 3\varepsilon_{\text{eq}}$ is the equilibrium value of ϕ_s in the rubbery state. Equation (7) is an ODE for $\phi_s(h_0, t)$, and can be solved easily. The solution of eq. (7) is shown in the inset of Figure 2(b). It is seen that $\phi_s(h_0, t)$ first increases slowly with time, and then shoots up to approach a steady state value $\phi_{\text{st}} = \phi_{\text{eq}}K/(K + (4/3)G)$ when it reaches the critical value ϕ_{cri} . The solution of eq. (6) under such time varying boundary condition gives the

profile of $\phi_s(z, t)$ in the induction period ($t < 0.5\tau_{\text{dif}}$) shown in Figure 2(b).

Such reasoning indicates that the induction time t_{ind} is given by the time during which the solution of eq. (7) increases from 0 to ϕ_{cri} , and is given by

$$t_{\text{ind}} \approx \frac{4}{3} \frac{\eta_g}{K} \frac{\phi_{\text{cri}}}{\phi_{\text{eq}}} \quad (8)$$

Equation (8) indicates that t_{ind} is essentially given by the rheological relaxation time of the glassy state $\tau_{\text{rhe}} = \eta_g/G$ since K and G are of the same order of magnitude in the glassy state. Equation (8) will be compared with numerical results later.

Case II diffusion period. The phenomena occurring at the gel surface in the induction period keep occurring at the front of the rubbery region, i.e., at the glassy side of the glass/rubber boundary, where the solvent supply from the rubbery side changes the glassy side to rubbery state. After the time of t_{ind} , the region of length $h_w^0 \simeq \sqrt{D_g t_{\text{ind}}}$ in the glassy side is changed to rubbery state, where $D_g = (K + \frac{4}{3}G)/\xi_g$ is the diffusion constant in the glassy side, and the front moves the distance h_w^0 . Therefore the front velocity v_{front} is given by h_w^0/t_{ind} , or

$$v_{\text{front}} \simeq \sqrt{\frac{D_g}{t_{\text{ind}}}} \simeq \sqrt{\frac{D_g K}{\eta_g}} \quad (9)$$

This scaling relation is consistent with the previous argument by Thomas and Windle model [15, 20, 38].

Figure 2(c) shows that at the end of the case II diffusion period, v_{front} starts to increase because the rubbery front coming from the two sides of the sample meets, and accelerate the permeation speed. When the solvent concentration at $z = 0$ exceeds ϕ_{cri} , the glassy region quickly disappears. The dynamics of this last stage will be discussed in the following.

Relaxation period. So far we have been discussing the motion in z direction (the transverse direction). We now discuss the motion in x and y direction (the lateral direction). Figure 3 shows the result of the numerical calculation for the transverse strain $\varepsilon_z = \Delta h(t)/h_0$ (black line) and the lateral strain $\varepsilon_x = \alpha(t)$ (red line), for two different parameter sets: Figure 3(a) is for $\eta_r/\xi_r h_0^2 = 0.005$ and Figure 3(b) is for larger viscosity, $\eta_r/\xi_r h_0^2 = 0.05$. It is seen that when the transverse strain $\Delta h(t)/h_0$ is increasing, the lateral strain α is also increasing. This is quite natural because when a gel is swelled, it expands in all directions. In the present situation, the lateral strain ε_x is much smaller than the transverse strain ε_z since the lateral expansion is constrained by the glassy region located at the center. In the middle of the case II diffusion period, ε_z becomes larger than the equilibrium value ε_{eq} , but ε_x remains much smaller than ε_{eq} . When the two rubbery regions meet at the center, ε_z starts to decrease and shows the undershoot, while ε_x

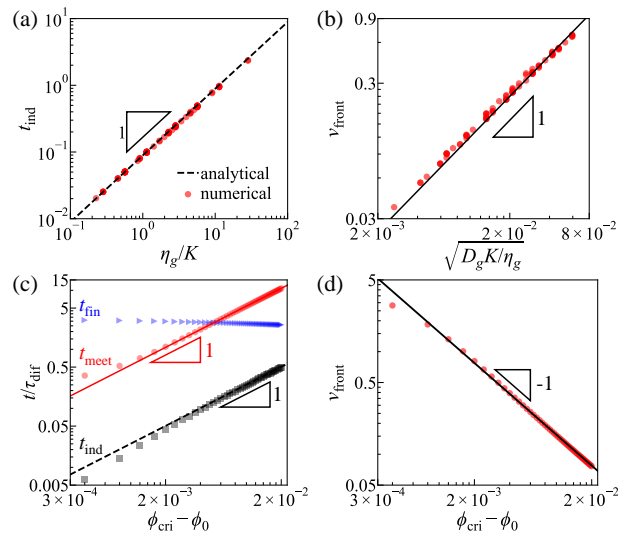


FIG. 4. (a) The dependence of induction time t_{ind} on material parameters η_g/K (in units of τ_{dif}). The black-dashed line is analytical solution of eq. (8) for $\phi_0 = 0$. (b) The dependence of the front velocity v_{front} on $\sqrt{D_g K/\eta_g}$ (in units of h_0/τ_{dif}) for $\phi_0 = 0$. (c) The dependence of induction time t_{ind} (black squares), case II diffusion time t_{meet} (red circle), and relaxation time t_{fin} (blue triangles) on $\phi_{\text{cri}} - \phi_0$. The black-dashed line is obtained by $t_{\text{ind}} = \frac{4}{3} \frac{\eta_g}{K} \frac{\phi_{\text{cri}} - \phi_0}{\phi_{\text{eq}}}$. (d) The dependence of the front velocity v_{front} (in units of h_0/τ_{dif}) (red circle) on $\phi_{\text{cri}} - \phi_0$. All data points are numerically calculated from the full model, while all solid lines are guiding lines.

keeps increasing. Such behaviors were reported in previous experiments [7], but no theoretical analysis has been done. Our theory is the first to explain the behavior in a single theoretical framework.

The time dependence of the thickness $\Delta h(t)$ is not simple: In the case of Figure 3(a), $\Delta h(t)$ shows overshoot and undershoot before it relaxes to the final equilibrium value, while in the case of Figure 3(b), $\Delta h(t)$ does not show such undershoot. Such distinction can be qualitatively explained as follows.

The relaxation of the volume strain $\varepsilon_z + 2\varepsilon_x$ is governed by the diffusion of solvent, which is characterized by the diffusion time τ_{dif} . On the other hand, the relaxation of shear strain is governed by the viscoelasticity of polymer in the rubbery state, which is characterized by the rheological relaxation time $\tau_{\text{rhe}} = \eta_r/G$. If η_r is small, the shear strain $\varepsilon_z - \alpha(t)$ quickly relaxes to zero, and the resulting isotropic strain $\varepsilon_z = \alpha(t)$ relaxes to the equilibrium value ε_{eq} with diffusion time τ_{dif} . This gives the behavior shown in Fig. 3(a). On the other hand, if η_r is large, ε_z and $\alpha(t)$ relax to their equilibrium values independently of each other with rheological relaxation time τ_{rhe} . This gives the behavior shown in Fig. 3(b).

Material parameter dependence. The case II diffusion is characterized by two physical quantities, the

induction time t_{ind} and the front velocity v_{front} . We have shown that if the sample includes no solvent initially, i.e., if ϕ_0 is zero, t_{ind} and v_{front} are given by eq. (8) and (9). Figure 4(a) and 4(b) show the comparison of these equations with numerical results. They confirm the validity of the scaling relations $t_{\text{ind}} \sim \eta_g/K$ and $v_{\text{front}} \sim \sqrt{D_g K/\eta_g}$.

Figure 4(c) shows how the characteristic times of the three periods change when the initial solvent volume fraction ϕ_0 is increased. It is seen that t_{ind} decreases with the increase of ϕ_0 in proportion to $\phi_{\text{cri}} - \phi_0$. Solving the boundary condition eq. (5) under the initial condition $\phi_s = \phi_0$ and the approximation $\eta(\phi_s) \simeq \eta_g$ and $\alpha = \phi_0/3$, we have $t_{\text{ind}} \approx \frac{4}{3} \frac{\eta_g}{K} \frac{\phi_{\text{cri}} - \phi_0}{\phi_{\text{eq}}}$. Figure 4(d) indicates that v_{front} increase with the increase of ϕ_0 satisfying the scaling relation $v_{\text{front}} \sim (\phi_{\text{cri}} - \phi_0)^{-1}$. This is not consistent with the argument to derive eq. (9), which gives the scaling relation $v_{\text{front}} \sim (\phi_{\text{cri}} - \phi_0)^{-1/2}$. This discrepancy arises from the inaccurate estimation for the precursor length h_w : previously we assumed that h_w is given by $\sqrt{D_g t_{\text{ind}}}$, which decreases with the increase of ϕ_0 . On the other hand, the numerical calculation indicates that h_w is almost independent of ϕ_0 , and is equal to h_w^0 [36]. If we use this result, v_{front} is estimated by h_w^0/t_{ind} that is

$$v_{\text{front}} \sim \sqrt{\frac{D_g K}{\eta_g}} \frac{1}{\phi_{\text{cri}} - \phi_0} \quad (10)$$

As far as we know there are no experimental reports on how the front velocity changes when the initial solvent volume fraction is changed. Eq. (10) is a prediction of our model, and it may be checked experimentally.

Figure 4(c) shows other characteristic times defined in Fig. 2(c): t_{meet} is the duration time of the case II diffusion stage, and t_{fin} is the relaxation time in the final relaxation stage. t_{meet} is estimated by h_0/v_{front} , and is therefore proportional to $\phi_{\text{cri}} - \phi_0$. t_{fin} is estimated by $t_{\text{fin}} \sim h_0^2/D_r$ and is independent of ϕ_0 . Such characteristic times depend on the sample thickness h_0 : t_{ind} is independent of h_0 , and t_{meet} and t_{fin} are proportional to h_0 and h_0^2 respectively. These relations are checked by the numerical calculation [36].

In summary, we proposed a continuum theory for the swelling of glassy polymer gels. The theory describes the three dimensional coupling between diffusion and viscoelasticity, and explains the classical experimental results found by Thomas and Windle. The theory gives predictions how the induction time and the front velocity depend on material parameters (diffusion constant and relaxation times) and sample condition (sample thickness and initial solvent concentration). These predictions can be checked experimentally.

Since the theory can describe the glass transition induced by solvent diffusion and mechanical forces, it may be used for a wider class of problems such as as plastic

deformation, membrane filtration and fracture or healing.

ASSOCIATED CONTENT

Supporting Information: detailed derivation of our theoretical model, and explanation on how we numerically obtain the front velocity and the characteristic times.

ACKNOWLEDGMENTS

We thank Hugues Chaté for useful discussions. This work was supported in part by the National Natural Science Foundation of China (NSFC) under grant No. 21961142020, the Fundamental Research Funds for the Central University under grant No. YWF-22-K-101. We also acknowledge the support of the High-Performance Computing Center of Beihang University.

* masao.doi@buaa.edu.cn

† manxk@buaa.edu.cn

- [1] Thomas, N.; Windle, A. Discontinuous shape changes associated with Case II transport of methanol in thin sheets of PMMA. *Polymer* **1977**, *18*, 1195
- [2] Alfrey Jr., T.; Gurnee, E. F.; Lloyd, W. G. Diffusion in glassy polymers. *J. polym. sci., C Polym. symp.* **1966**, *12*, 249–261
- [3] Sanopoulou, M.; Petropoulos, J. H. Systematic Analysis and Model Interpretation of Micromolecular Non-Fickian Sorption Kinetics in Polymer Films. *Macromolecules* **2001**, *34*, 1400–1410
- [4] Ji, S.; Ding, J. The Wetting Process of a Dry Polymeric Hydrogel. *Polym. J.* **2002**, *34*, 267–270
- [5] De Kee, D.; Liu, Q.; Hinestroza, J. Viscoelastic (Non-Fickian) Diffusion. *Can. J. Chem. Eng.* **2005**, *83*, 913–929
- [6] Petropoulos, J. H.; Sanopoulou, M.; Papadokostaki, K. G. Physically insightful modeling of non-Fickian kinetic regimes encountered in fundamental studies of isothermal sorption of swelling agents in polymeric media. *Eur. Polym. J.* **2011**, *47*, 2053–2062
- [7] Thomas, N. L.; Windle, A. H. Diffusion mechanics of the system PMMA-methanol. *Polymer* **1981**, *22*, 627–639
- [8] Lasky, R. C.; Kramer, E. J.; Hui, C.-Y. Temperature dependence of case II diffusion. *Polymer* **1988**, *29*, 1131–1136
- [9] Foreman, M. R.; Vollmer, F. Optical Tracking of Anomalous Diffusion Kinetics in Polymer Microspheres. *Phys. Rev. Lett.* **2015**, *114*, 118001
- [10] Nixdorf, J.; Di Florio, G.; Bröckers, L.; Borbeck, C.; Hermes, H. E.; Egelhaaf, S. U.; Gilch, P. Uptake of Methanol by Poly(methyl methacrylate): An Old Problem Addressed by a Novel Raman Technique. *Macromolecules* **2019**, *52*, 4997–5005

- [11] Bischak, C. G.; Flagg, L. Q.; Yan, K.; Rehman, T.; Davies, D. W.; Quezada, R. J.; Onorato, J. W.; Luscombe, C. K.; Diao, Y.; Li, C.-Z.; Ginger, D. S. A Reversible Structural Phase Transition by Electrochemically-Driven Ion Injection into a Conjugated Polymer. *J. Am. Chem. Soc.* **2020**, *142*, 7434–7442
- [12] Hausmann, B. D.; Tomozawa, M. Case II diffusion of water in Na₂O-3SiO₂ glass: Constant tensile stress gradient at the diffusion interface. *Int. J. Appl. Glass Sci.* **2023**, *14*, 330–337
- [13] Thomas, N. L.; Windle, A. H. A deformation model for Case II diffusion. *Polymer* **1980**, *21*, 613–619
- [14] Rossi, G.; Pincus, P. A.; de Gennes, P.-G. A Phenomenological Description of Case-II Diffusion in Polymeric Materials. *Europhys. Lett.* **1995**, *32*, 391
- [15] Qian, T.; Taylor, P. From the Thomas-Windle model to a phenomenological description of Case-II diffusion in polymers. *Polymer* **2000**, *41*, 7159–7163
- [16] Bargmann, S.; McBride, A. T.; Steinmann, P. Models of Solvent Penetration in Glassy Polymers With an Emphasis on Case II Diffusion. A Comparative Review. *Appl. Mech. Rev.* **2011**, *64*, 010803
- [17] Miao, J.; Tsige, M.; Taylor, P. L. Generalized model for the diffusion of solvents in glassy polymers: From Fickian to Super Case II. *J. Chem. Phys.* **2017**, *147*, 044904
- [18] Borrmann, D.; Danzer, A.; Sadowski, G. Generalized Diffusion-Relaxation Model for Solvent Sorption in Polymers. *Ind. Eng. Chem. Res.* **2021**, *60*, 15766–15781
- [19] Song, Z.; Li, X.; Wu, K.; Cai, S. Nonequilibrium thermodynamic modeling of case II diffusion in glassy polymers. *J. Mech. Phys. Solids* **2023**, *179*, 105395
- [20] Thomas, N.; Windle, A. A theory of case II diffusion. *Polymer* **1982**, *23*, 529–542
- [21] Kalospiros, N. S.; Ocone, R.; Astarita, G.; Meldon, J. H. Analysis of anomalous diffusion and relaxation in solid polymers. *Ind. Eng. Chem. Res.* **1991**, *30*, 851–864
- [22] Jou, D.; Camacho, J.; Grmela, M. On the nonequilibrium thermodynamics of non-Fickian diffusion. *Macromolecules* **1991**, *24*, 3597–3602
- [23] Lustig, S.; Caruthers, J.; Peppas, N. Continuum thermodynamics and transport theory for polymer—fluid mixtures. *Chem. Eng. Sci.* **1992**, *47*, 3037–3057
- [24] Govindjee, S.; Simo, J. C. Coupled stress-diffusion: Case II. *J. Mech. Phys. Solids* **1993**, *41*, 863–887
- [25] Wilmers, J.; Bargmann, S. A continuum mechanical model for the description of solvent induced swelling in polymeric glasses: Thermomechanics coupled with diffusion. *Eur. J. Mech. A-Solid* **2015**, *53*, 10–18
- [26] Krenn, P.; Zimmermann, P.; Fischlschweiger, M.; Zeiner, T. SAFT-Based Maxwell-Stefan Approach to Model the Diffusion through Epoxy Resins. *J. Chem. Eng. Data* **2020**, *65*, 5677–5687
- [27] Crank, J. *The Mathematics of Diffusion*; Oxford University Press, 1975
- [28] Carbonell, R. G.; Sarti, G. C. Coupled deformation and mass-transport processes in solid polymers. *Ind. Eng. Chem. Res.* **1990**, *29*, 1194–1204
- [29] Doi, M. Gel dynamics. *J. Phys. Soc. Jpn.* **2009**, *78*, 052001
- [30] Man, X.; Doi, M. Swelling Dynamics of a Disk-Shaped Gel. *Macromolecules* **2021**, *54*, 4626–4632
- [31] Ding, Z.; Lyu, P.; Shi, A.; Man, X.; Doi, M. Diffusio-Mechanical Theory of Gel Bending Induced by Liquid Penetration. *Macromolecules* **2022**, *55*, 7092–7099
- [32] Lyu, P.; Ding, Z.; Man, X. Accelerating the stimulative bending of a gel using mechanical constraints. *Eur. Phys. J. E* **2023**, *46*, 40
- [33] Doi, M. *Soft Matter Physics*; Oxford University Press, 2013
- [34] Doi, M. Onsager principle in polymer dynamics. *Prog. Polym. Sci.* **2021**, *112*, 101339
- [35] Ferry, J. D. *Viscoelastic Properties of Polymers*; John Wiley & Sons, 1980
- [36] see supporting information
- [37] Tanaka, T.; Fillmore, D. J. Kinetics of swelling of gels. *J. Chem. Phys.* **1979**, *70*, 1214–1218
- [38] Hui, C.-Y.; Wu, K.-C.; Lasky, R. C.; Kramer, E. J. Case-II diffusion in polymers. II. Steady-state front motion. *J. Appl. Phys.* **1987**, *61*, 5137–5149

for Table of Contents use only

A Unified Model for Non-Fickian Diffusion and Anomalous Swelling of Glassy Polymer Gels

Peihan Lyu, Zhaoyu Ding, Masao Doi, Xingkun Man**

